N89-21759

1988

NASA/ASEE SUMMER FACULTY FELLOWSHIP PROGRAM

MARSHALL SPACE FLIGHT CENTER
THE UNIVERSITY OF ALABAMA

Rotordynamic Analysis of a Bearing Tester

Prepared by: Richard A. Zalik

Academic Rank: Professor

University and Department: Auburn University

Department of Algebra,
Combinatorics and Analysis

NASA/MSFC

Laboratory: Structures and Dynamics
Division: Control Systems
Branch: Mechanical Systems Control

MSFC Colleague: Thomas H. Fox

Date: August 30, 1988

Contract No.: NGT 01-002-099
The University of Alabama

Rotordynamic Analysis of a Bearing Tester

R. A. Zalik

Auburn University
Division of Mathematics
120 Mathematics Annex Building
Auburn, AL 36849-5307

Acknowledgement

This work was written at Marshall Space Flight Center with the support of a NASA/ASEE Faculty Fellowship. The author would like to thank NASA for the use of their facilities, and acknowledge with gratitude the assistance of several MSFC personnel, in particular P. Broussard, T. H. Fox, G. von Pragenau, S. Ryan and J. Slaby.

Objectives

The objective of this paper is to study the stability characteristics of a bearing tester. We verify our conclusions using numerical simulations of a realistic model.

Abstract. We study the properties of the solutions of a system of four coupled nonlinear differential equations that model the behavior of the rotating shaft of a bearing tester. In particular, we show how bounds for the solutions of these equation can be obtained from bounds for the solutions of the linearized equations. By studying the behavior of the Fourier transforms of the solutions, we are also able to predict the approach to the stability boundary. These conclusions are verified by means of numerical solutions of the equations, and of power spectrum density (PSD) plots.

1. Introduction.

In this study we continue the investigation of the properties of the solutions of mathematical models of rotating machinery initiated by Day [1]. Both Day and this author [2] have studied the behavior of a simple Jeffcott model with deadband, viz. a system of coupled differential equations that represent the behavior of a rotating shaft.

The purpose of this paper is to examine the properties of the solutions of a model of a bearing tester. This is a device designed to estimate the life expectancy of bearings under realistic conditions of loads and acceleration in cryogenic fluids. Our study will help determine safety margins for its operation.

We consider a bearing tester with two seals and two bearings with deadband. A sketch of this mechanical system can be seen in Fig. 1.

2. General Theory

2.1 Derivation of the Bearing Tester Equations.

We assume that the shaft is rotating with angular velocity ω along an axis close to the x-axis, that both bearings are at the same distance a from the center of symmetry of the shaft, that both seals are at the same distance b from this center of symmetry, and that the shaft cannot move in the direction of the x-axis. We also assume that both seals have the same damping C_s, stiffness K_s, and cross coupling stiffness Q_s, and that both bearings have the same stiffness K_b.

For $j = 1, 2$, let δ_j denote the magnitude of the deadband at bearing j; let v_{yj} and v_{zj} describe the displacement of the center of the shaft at bearing j, and let w_{yj} and w_{zj} be similarly defined for the seals (see Fig. 2). Let m denote the mass of the shaft. If $r_j = (v_{yj}^2 + v_{zj}^2)^{1/2}$,

$h_j(t) = 1$ if $r_j \leq \delta_j$, and $h_j(t) = \delta_j/r_j$ if $r_j > \delta_j$, then the equations that describe the movement of the shaft are the following:

$$K_b[1-h_1(t)]v_{y1} + K_b[1-h_2(t)]v_{y2} + K_s[w_{y1} + w_{y2}] + Q_s[w_{z1} + w_{z2}] + C_s[w'_{y1} + w'_{y2}] + (m/2)[v''_{y1} + v''_{y2}] = g_1(t) \quad (1)$$

$$K_b[1-h_1(t)]v_{z1} + K_b[1-h_2(t)]v_{z2} + K_s[w_{z1} + w_{z2}] - Q_s[w_{y1} + w_{y2}] + C_s[w'_{z1} + w'_{z2}] + (m/2)[v''_{z1} + v''_{z2}] = g_2(t) \quad (2)$$

$$-aK_b[1-h_1(t)]v_{y1} + aK_b[1-h_2(t)]v_{y2} + bK_s[w_{y2} - w_{y1}] + bQ_s[w_{z2} - w_{z1}] + bC_s[w'_{y2} - w'_{y1}] + (I_2/2a)[v''_{y2} - v''_{y1}] - (\omega I_1/2a)[v'_{z2} - v'_{z1}] = m_1(t) \quad (3)$$

$$-aK_b[1-h_1(t)]v_{z1} + aK_b[1-h_2(t)]v_{z2} + bK_s[w_{z2} - w_{z1}] - bQ_s[w_{y2} - w_{y1}] + bC_s[w'_{z2} - w'_{z1}] + (I_2/2a)[v''_{z2} - v''_{z1}] + (\omega I_1/2a)[v'_{y2} - v'_{y1}] = m_2(t) \quad (4)$$

$$v_{y1} + v_{y2} = w_{y1} + w_{y2}, \qquad v_{z1} + v_{z2} = w_{z1} + w_{z2} \quad (5)$$

$$v_{y1} - v_{y2} = w_{y1} - w_{y2}, \qquad v_{z1} - v_{z2} = w_{z1} - w_{z2}, \quad (6)$$

where I_1 is the axial inertia, I_2 is the rotational inertia about the axis transversal to the shaft, and $g_1(t)$, $g_2(t)$, $m_1(t)$, $m_2(t)$ are given as follows:

$$g_1(t) = \omega^2 m[(e_{y1} + e_{y2})\cos \omega t - (e_{z1} + e_{z2}) \sin \omega t]$$

$$g_2(t) = \omega^2 m[(e_{z1} + e_{z2})\cos \omega t + (e_{y1} + e_{y2}) \sin \omega t]$$

$$m_1(t) = \omega^2 m[(e_{y1} - e_{y2}) \cos \omega t - (e_{z1} - e_{z2}) \sin \omega t]$$

$$m_2(t) = \omega^2 m[(e_{z1} - e_{z2}) \cos \omega t + (e_{y1} - e_{y2}) \sin \omega t],$$

where e_{y1}, e_{y2}, e_{z1} and e_{z2} represent the mass imbalance. In our analyses we shall assume that g_1, g_2, m_1, and m_2 are arbitrary continuous and bounded functions.

Note that (1) and (2) are force equations, (3) and (4) are moment equations, and (5) and (6) are derived from the symmetry assumptions on bearings and seals. Setting $v_j = v_{yj} + iv_{zj}$, $w_j = w_{yj} + iw_{zj}$, $g(t) = g_1(t) + ig_2(t)$ and $m(t) = m_1(t) + im_2(t)$, we obtain:

$$K_b[1-h_1(t)]v_1 + K_b[1-h_2(t)]v_2 + (K_s - iQ_s)[w_1 + w_2] + C_s[w_1' + w_2'] + (m/2)[v_1'' + v_2''] = g(t). \tag{7}$$

$$-aK_b[1-h_1(t)]v_1 + aK_b[1-h_2(t)]v_2 + b(K_s - iQ_s)[w_2 - w_1] + bC_s[w_2' - w_1'] + (I_2/2a)[v_2'' - v_1''] + i(\omega I_1/2a)[v_2' - v_1'] = m(t), \tag{8}$$

and

$$v_1 + v_2 = w_1 + w_2, \qquad v_1 - v_2 = w_1 - w_2 \tag{9}$$

In view of (9), if we set $v = v_1 + v_2$, $u = v_2 - v_1$, $q_1 = h_1v_1$, and $q_2 = h_2v_2$, (7) and (8) can be written in the following form:

$$(m/2)v'' + C_sv' + (K_b + K_s - iQ_s)v - K_b[q_1 + q_2] = g(t),$$

and

$$(I_2/2a)u'' + (bC_s + i\omega I_1/2a)u' + (aK_b + bK_s - ibQ_s)u + aK_b[q_1 - q_2] = m(t).$$

Thus, setting $C_1 = 2C_s/m$, $C_2 = (2abC_s + i\omega I_1)/I_2$, $K_1 = 2K_b/m$, $K_2 = (2a^2K_b)/I_2$, $A_1 = 2K_s/m$, $A_2 = 2abK_s/I_2$, $B_1 = 2Q_s/m$, $B_2 = 2abQ_s/I_2$, $M_1 = A_1 + K_1 - iB_1$,

$M_2 = A_2 + K_2 - iB_2$, $f_1(t) = (2/m)\, g(t)$, $f_2(t) = (2a/I_2)m(t)$, and

$$p_1 = q_1 + q_2, \qquad p_2 = q_1 - q_2, \tag{10}$$

we finally obtain the Bearing Tester equations:

$$v'' + C_1 v' + M_1 v - K_1 p_1 = f_1(t), \tag{11}$$

and

$$u'' + C_2 u' + M_2 u + K_2 p_2 = f_2(t). \tag{12}$$

We shall assume that B_1, B_2, C_1, C_2, K_1, K_2, δ_1, δ_2 are positive, and A_1, A_2 and t are nonnegative.

Since $v_1 = (1/2)(v - u)$ and $v_2 = (1/2)(v + u)$, $p_1(t)$ and $p_2(t)$ can be expressed in terms of v and u using (10) and the following representations for $q_1(t)$ and $q_2(t)$:

$$q_1(t) = \begin{cases} (v-u)/2, & \text{if } |v-u| \le 2\delta_1 \\ \delta_1(v-u)/|v-u|, & \text{if } |v-u| > 2\delta_1 \end{cases}, \tag{13}$$

and

$$q_2(t) = \begin{cases} (v+u)/2, & \text{if } |v+u| \le 2\delta_2 \\ \delta_2(v+u)/|v+u|, & \text{if } |v+u| > 2\delta_2. \end{cases} \tag{14}$$

2.2 Existence, uniqueness, and representation formulas.

We have transformed the system of equations (1) - (6) into the equivalent system (11), (12). This is a system of coupled nonlinear differential equations similar to the Jeffcott equations we studied in [2]. The existence and uniqueness of their solutions (and therefore, of the solutions of the original system), follow by the same argument employed for the Jeffcott equations, and need not be repeated here.

Let $Q_1 = C_1^2 - 4(A_1 + K_1)$,

$$\beta_1 = 8^{-1/2}[-Q_1 + (Q_1^2 + 16B_1^2)^{1/2}]^{1/2}, \tag{15}$$

$$\alpha_1 = [\beta_1^{-1}B_1 - C_1]/2, \qquad \alpha_1' = -[\beta_j^{-1}B_1 + C_1]/2, \tag{16}$$

$$\lambda_1 = \alpha_1 + i\beta_1, \qquad \lambda_2 = \alpha_1' - i\beta_1. \tag{17}$$

Then, as in [2], it is readily seen that λ_1 and λ_2 are the solutions of the characteristic equation $\lambda^2 + C_1\lambda + M_1 = 0$, and therefore

$$v_h = c_1 \exp(\lambda_1 t) + c_2 \exp(\lambda_2 t) \tag{18}$$

is the general solution of

$$v'' + C_1 v' + M_1 v = 0, \tag{19}$$

Similarly, if $\gamma_1 = \alpha_2 + i\beta_2$ and $\gamma_2 = \alpha_2' + i\beta_2'$ are the solutions of the characteristic equation $\gamma^2 + C_2\gamma + M_2 = 0$, it is clear that

$$u_h = d_1 \exp(\gamma_1 t) + d_2 \exp(\gamma_2 t) \tag{20}$$

is the general solution of

$$u'' + C_2 u' + M_2 u = 0. \tag{21}$$

Without loss of generality, we shall always assume that $\alpha_2' \leq \alpha_2$. If C_2 is real (i.e., if $\omega I_1 = 0$), then formulas similar to (15), (16) and (17) obtain for γ_1 and γ_2.

If v_p and u_p are particular solutions of the linearlized Bearing Tester equations

$$v'' + C_1 v' + M_1 v = f_1(t) \tag{22}$$

and

$$u'' + C_2 u' + M_2 u = f_2(t), \tag{23}$$

then, setting $v_\ell = v_h + v_p$, $u_\ell = u_h + u_p$,

$$G_1(t) = (\lambda_1 - \lambda_2)^{-1}[\exp(\lambda_1 t) - \exp(\lambda_2 t)],$$

$$G_2(t) = (\gamma_1 - \gamma_2)^{-1}[\exp(\gamma_1 t) - \exp(\gamma_2 t)],$$

and proceeding as in [2], we readily deduce that (11) and (12) are equivalent to the following nonlinear Volterra integral equations of convolution type:

$$v(t) = v_\ell(t) + P_1(t) \tag{24}$$

and

$$u(t) = u_\ell(t) + P_2(t), \tag{25}$$

where the perturbation terms $P_j(t)$ are given by:

$$P_j(t) = K_j \int_0^t G_j(t-x)p_j(x)dx, \quad j = 1, 2. \tag{26}$$

Thus, the existence and uniqueness of the solutions of (11) and (12) also follow from the existence and uniqueness of the solutions of (24) and (25) (cf. e.g. [3], [4]).

2.2 Bounds

Let $D_j(t) = \int_o^t \left|G_j(t-x)\right| dx$, and let $\delta = \delta_1 + \delta_2$. Since (10), (11), (13) and (14) imply that

$$\left|p_j(t)\right| \leq \delta, \quad j = 1, 2, \tag{27}$$

we readily conclude that

$$\left|P_j(t)\right| \leq \delta K_j D_j(t), \quad j = 1, 2 \tag{28}$$

Let $D_1 = \left|\lambda_1 - \lambda_2\right|^{-1} \left(\left|\alpha_1\right|^{-1} + \left|\alpha_1'\right|^{-1}\right)$, $D_2 = \left|\gamma_1 - \gamma_2\right|^{-1} \left(\left|\alpha_2\right|^{-1} + \left|\alpha_2'\right|^{-1}\right)$. Note that $\alpha_j' \leq \alpha_j$. Thus if $\alpha_j < 0$ we readily see that D_j is a steady state bound for $D_j(t)$. From these inequalities we derive, as in [2], the following conclusions:

1. If $\alpha_1 < 0$ and $\left|v_p\right| \leq M_1$, then the steady state solution v_∞ of (11) satisfies the following inequality:

   $$\left|v_\infty\right| \leq M_1 + \delta K_1 D_1$$

   whereas if $\alpha_2 < 0$ and $\left|u_p\right| \leq M_2$, the steady state solution u_∞ of (12) satisfies the inequality

   $$\left|u_\infty\right| \leq M_2 + \delta K_2 D_2$$

2. If $\alpha_j = 0$, the perturbation term $P_j(t)$ can grow at most linearly.
3. If $\alpha_j > 0$, the order of growth of $P_j(t)$ cannot exceed $\exp(\alpha_j t)$; note that the order or magnitude of all nonzero solutions of (19) or

(21) cannot exceed $\exp(\alpha_j t)$.

Since our assumptions imply that $f_1(t)$ and $f_2(t)$ are bounded, we have therefore shown that the study of the boundedness of the solutions of (11) or (12) reduces to the study of the boundedness of the solutions of (19) or (21).

If $\alpha_1 < 0$ and $\alpha_2 < 0$ we shall say that the system (11), (12) (or (1)-(6)) is stable, if $\alpha_1 = 0$ and $\alpha_2 \leq 0$, or $\alpha_1 \leq 0$ and $\alpha_2 = 0$, that the system has reached the stability boundary, and if $\alpha_1 > 0$ or $\alpha_2 > 0$, that the system is unstable. Thus the system is stable if all its solutions are bounded.

2.3. Estimates for β_1 and β_2

We obtain estimates for the β_j in terms of the coefficients of (11) and (12) and the signs of the α_j. These estimates yield a simple method for determining the stability of the system. Since (19) is identical with [2, (7)], we know the following:

1. If $\alpha_1 < 0$, then $B_1/C_1 < \beta_1 < (A_1 + K_1)^{1/2}$, and $\alpha_1' < 0$.
2. If $\alpha_1 = 0$, then $B_1/C_1 = \beta_1 = (A_1 + K_1)^{1/2}$, and $\alpha_1' < 0$.
3. If $\alpha_1 > 0$, then $(A_1 + K_1)^{1/2} < \beta_1 < B_1/C_1$.

If C_2 is real (i.e., if $\omega I_1 = 0$), we also have:

4. If $\alpha_2 < 0$, then $B_2/C_2 < \beta_2 < (A_2 + K_2)^{1/2}$, and $\alpha_2' < 0$.
5. If $\alpha_2 = 0$, then $B_2/C_2 = \beta_2 = (A_2 + K_2)^{1/2}$, and $\alpha_2' < 0$.
6. If $\alpha_2 > 0$, then $(A_2 + K_2)^{1/2} < \beta_2 < B_2/C_2$.

From these conclusions we also infer that if $f_1(t)$ and $f_2(t)$ are bounded, and $I_1 = 0$, then the system (1) - (6) is stable if and only if

$B_1/C_1 < (A_1 + K_1)^{1/2}$, and $B_2/C_2 < (A_2 + K_2)^{1/2}$.

2.4 Resonance

Proceeding as in [2], we readily see that if $f_j(t) = A_j \exp(iwt)$, $j = 1, 2$, then (1) - (6) can be in resonance only if $\alpha = 0$ or $Q_s/C_s = [2a(bK_s + aK_b)/(I_1 + I_2)]^{1/2}$.

3. Harmonic Analysis of the solutions.

3.1. Preliminaries.

We now study the properties of the Fourier transforms of the solutions. Following standard practice, we consider a time interval of the form (c, d) $0 \leq c < d < \infty$. Let $g^{(c,d)}(t) = g(t)$ if $c \leq t \leq d$, and let $g^{(c,d)}(t) = 0$ otherwise. Thus, if F denotes the Fourier transform operator, we have:

$$F[g^{(c,d)}](s) = (2\pi)^{-1/2} \int_c^d g(t) \exp(ist)dt,$$

and proceeding as in [2] we see that

$$\lim_{c\to\infty} F[v_h^{(c,d)}](s) = 0, \text{ and } \lim_{c\to\infty} F[u_h^{(c,d)}](s) = 0, \tag{29}$$

and therefore

$$\lim_{c\to\infty} F[v_1^{(c,d)}](s) = 0, \text{ and } \lim_{c\to\infty} F[v_2^{(c,d)}](s) = 0, \tag{30}$$

We want to study the properties of the graphs of the absolute values of $F[v^{(c,d)}](s)$ and $F[u^{(c,d)}](s)$. From (29) it is clear that in order to obtain useful information we need to study the Fourier transforms of the perturbation terms $P_j(t)$.

3.2. Analysis of the perturbation terms.

Let $Q_1(t) = \int_o^t \exp[\lambda_1(t-x)]p_1(x)dx$, and

$R_2(t) = \int_o^t \exp[\lambda_2(t-x)]p_1(x)dx$, and let $Q_2(t)$, $R_2(t)$ be similarly defined in terms of γ_1, γ_2, and $p_2(x)$. Clearly

$$p_1^{(c,d)}(t) = K_1(\lambda_1-\lambda_2)^{-1}[Q_1^{(c,d)}(t) - R_1^{(c,d)}(t)].$$

We have:

$$F[Q_1^{(c,d)}] = (2\pi)^{-1/2} \int_c^d \int_o^t \exp[\lambda_1(t-x)]p_1(x)dx \exp(-sti)dx$$

$$= (2\pi)^{-1/2} \int_c^d \int_o^t \exp(-\lambda_1 x)p_1(x)dx \exp[t(\lambda_1 - si)]dt,$$

and integrating by parts we obtain:

$$F[Q_1^{(c,d)}](s) =$$

$$(2\pi)^{-1/2}(\lambda_1-si)^{-1/2}[\exp(-dsi)p_1(d) - \exp(-csi)p_1(c)] - \int_c^d \exp(-s(i)p_1(t)dt]$$

$$= M_1(S, c, d)/(\lambda_1 - si),$$

where, since $|p_1(t)| \leq \delta$,

$$|M_1(s, c, d)| \leq (2\pi)^{-1/2}(2 + d - c)\delta. \qquad (31)$$

Using the same argument we also see that

$$F[R_1^{(c,d)}](s) = M_2(s, c, d)/\lambda_2 - si),$$

where $M_2(s, c, d)$ satisfies an inequality similar to (31). Thus,

$$F[p_1^{(c,d)}](s) = K_1(\lambda_1 - \lambda_2)^{-1}[M_1(s, c, d)/(\lambda_1-si) - M_2(s, c, d)/(\lambda_2 - si)]. \qquad (32)$$

Similarly,

$$F[P_2^{(c,d)}](s) = K_2(\gamma_1-\gamma_2)^{-1}[M_3(s, c, d)/(\gamma_1-si) - M_4(s, c, d)/(\gamma_2-si)], \qquad (33)$$

where $|M_3(s, c, d)|$ and $|M_4(s, c, d)|$ are bounded by $(2\pi)^{-1/2}(2+d-c)\delta$. Note, moreover, that there is no reason why $M_1(s, c, d)$ or $M_3(s, c, d)$ should vanish as $c \to \infty$, provided we keep the difference $d-c$ constant.

Since $v_1 = (1/2)(v-u)$ and $v_2 = (1/2)(v+u)$, for $j = 1, 2$ we obtain:

$$v_j = T_j + L_j + H_j,$$

where L_j is a particular solution of (7) or (8), $\lim_{c\to\infty} F[T_j^{(c,d)}](s) = 0$,

$$F[H_1^{(c,d)}](s) = (1/2)(F[p_1^{(c,d)}](s) - F[p_2^{(c,d)}](s)), \tag{34}$$

and

$$F[H_2^{(c,d)}](s) = (1/2)(F[p_1^{(c,d)}](s) + F[p_2^{(c,d)}](s)). \tag{35}$$

Since $\lambda_1 - si = \alpha_1 + (\beta_1 - si)$, and $\gamma_1 - si = \alpha_2 + (\beta_2 - si)$, this means that the only value for which $F[H_1^{(c,d)}](s)$ and $F[H_1^{(c,d)}](s)$ may diverge as $\alpha_1 \to 0^-$ is $s = \beta_1$, and the only value for which they may diverge as $\alpha_2 \to 0^-$ is $s = \beta_2$.

Let $\sigma = \max\{\alpha_1, \alpha_2\}$. We identify the nonlinear natural frequency with those frequencies at which the PSD plots have relative maxima that become unbounded $\sigma \to 0^-$. The method we have used to reach the conclusions of this section is much simpler than the one we employed in [2].

3.3.3 Conclusions

If $\sigma = \max\{\alpha_1, \alpha_2\}$ and $\xi = \beta$ if $\sigma = \alpha$ or $\xi = \beta_2$ otherwise, we conclude that as $\sigma \to 0$ $F[v_1^{(c,d)}](s)$ and $F[v_2^{(c,d)}](s)$ may diverge only at $s = \xi$ (or, if both $\alpha_1 \to 0^-$ and $\alpha_2 \to 0^-$ simultaneously, at both β and β'), that for σ negative and constant, but sufficiently close to zero, the graphs of the absolute values of $F[v_j(c,d)](s)$, $j = 1, 2$ will have spikes near $s = \xi$ (or, in PSD plots, near $\xi/s\pi$), and that the magnitudes of these spikes need not decrease with time (i.e., as $c \to \infty$).

4. Examples

We now study the behavior of the solutions of (11), (12) for various rotating speeds. We assume that $I_1 = 0$, $I_2 = 1.65$ lbf.in.sec^2, $\delta = 0.0015$ in., $m = 0.0587$ lb.sec^2/in., $a = 4.15$ in., $b = 7.1$ in. If ϕ denotes the angular

speed of the shaft in Hz., then $K_s = 0.0398\phi$ lb/in, $Q_s = 0.0201\phi$ lb/in, $C_s = 0.00001361$lb/in, and $K_b = -1{,}800\phi + 105{,}480{,}000$. We also assume that $e_{y1} = 5.7 \times 10^{-6}$ lb.sec^2/in, $e_{y2} = -e_{y1}$, $e_{z1} = e_{z2} = 0$, $v(0) = u(0) = \delta$, and $v'(0) = u'(0) = 1$. These values have been obtained from an actual bearing tester. Since, as we have already shown, when $\alpha_1 = 0$ we have $B_1/C_1 = (A_1 + K_1)^{1/2}$, we readily see that the value of ϕ for which this happens is $\phi_{c1} = 939$ Hz. = 56,359 rpm, and that $\alpha_1 < 0$ if $\phi < \phi_{c1}$. Since $I_1 = 0$, we can apply a similar procedure to conclude that $\phi_{c2} = 916$ Hz. = 54,950 rpm, and that $\alpha_2 < 0$ if $\phi < \phi_{c2}$. If f_1 denotes the frequency that corresponds to the value of β_1 when $\alpha_1 = 0$, it is readily seen that $\phi_1 = 245$ Hz. If f_2 denotes the frequency that corresponds to β_2 when $\alpha_2 = 0$, we see that also $\phi_2 = 245$ Hz. Since α_2 vanishes before α_1, we reach the stability boundary when the shaft's rotating speed is 54,950 rpm.

In Figs. 3 through 8 we see PSD plots for v_2 for various values of ϕ ranging from 30,000 rpm to 57,000 rpm. (The plots for v_1 are similar). To obtain these plots we first solved (11), (12) using a fourth order Runge-Kutta method. We then applied a Fast Fourier algorithm. The plots were obtained using 256 points and linear interpolation, and are for the time interval $5.120 \text{ sec.} < t < 5.632 \text{ sec.}$ The frequencies are measured in Hz.

Since the mass imbalance is so small, the forcing frequency ϕ is

undetectable. We see that as ϕ increases, the location of the nonlinear natural frequency σ remains at 246 Hz. The magnitude of the spike increases steadily, until around 50,000 rpm it starts to climb steeply. These examples show that the nonlinear natural frequency may appear well before the stability boundary is reached. They also show that the location of this frequency is not a good indicator of stability margins, and that the approach to the stability boundary is accompanied by a steep increase in the size of the spike. These conclusions are similar to those we reached for a simple Jeffcott model in [2].

References

1. W. B. Day, Asymptotic Expansions in Nonlinear Rotordynamics, Quart. Appl. Math. 44 (1987), 779-792.

2. R. A. Zalik, The Jeffcott Equations in Nonlinear Rotordynamics, Quart. Appl. Math., (to appear).

3. T. L. Saaty, "Modern Nonlinear Equations", Dover, New York, 1981.

4. F. G. Tricomi, "Integral Equations", Interscience, New York, 1957.

FIGURES

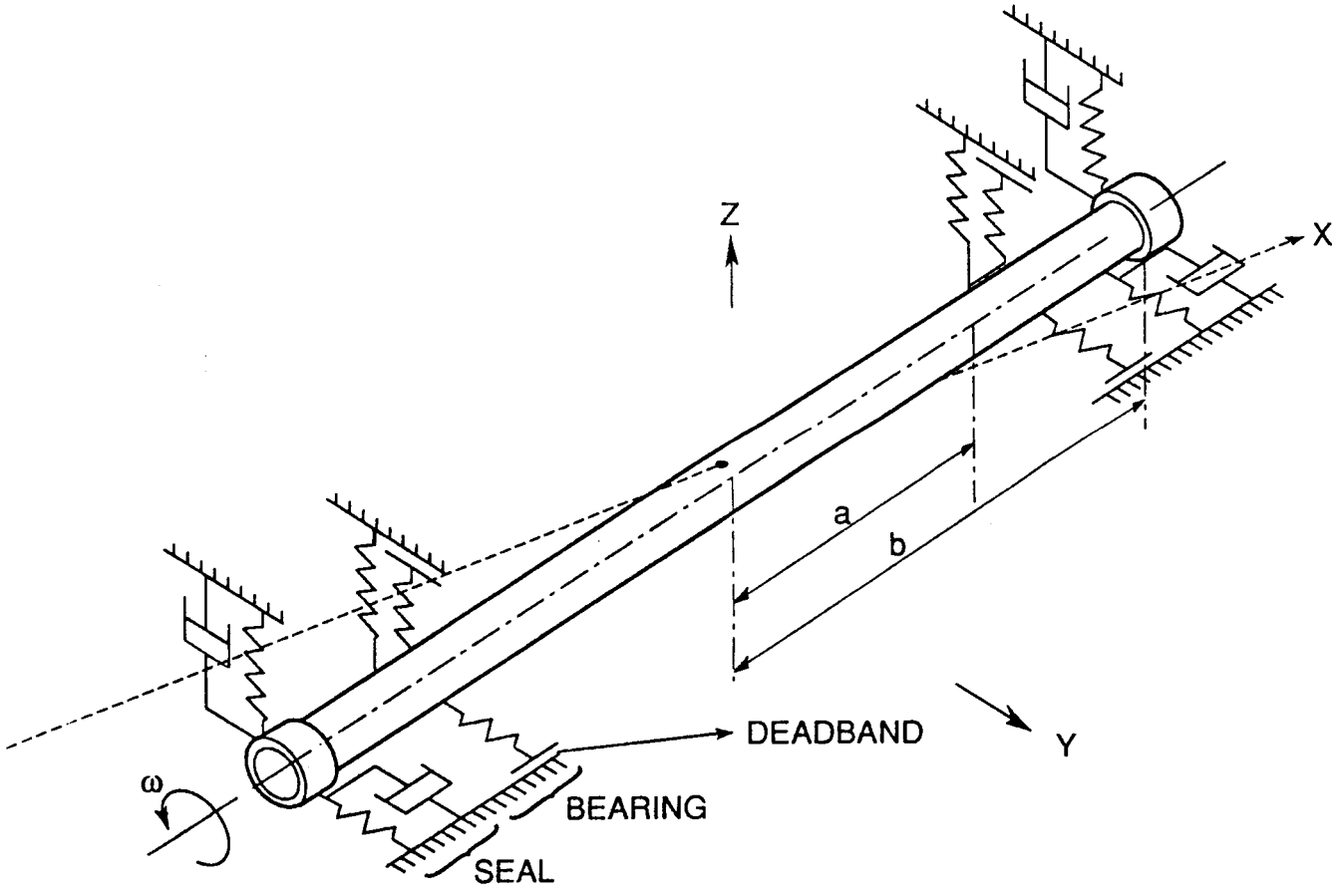

FIGURE 1

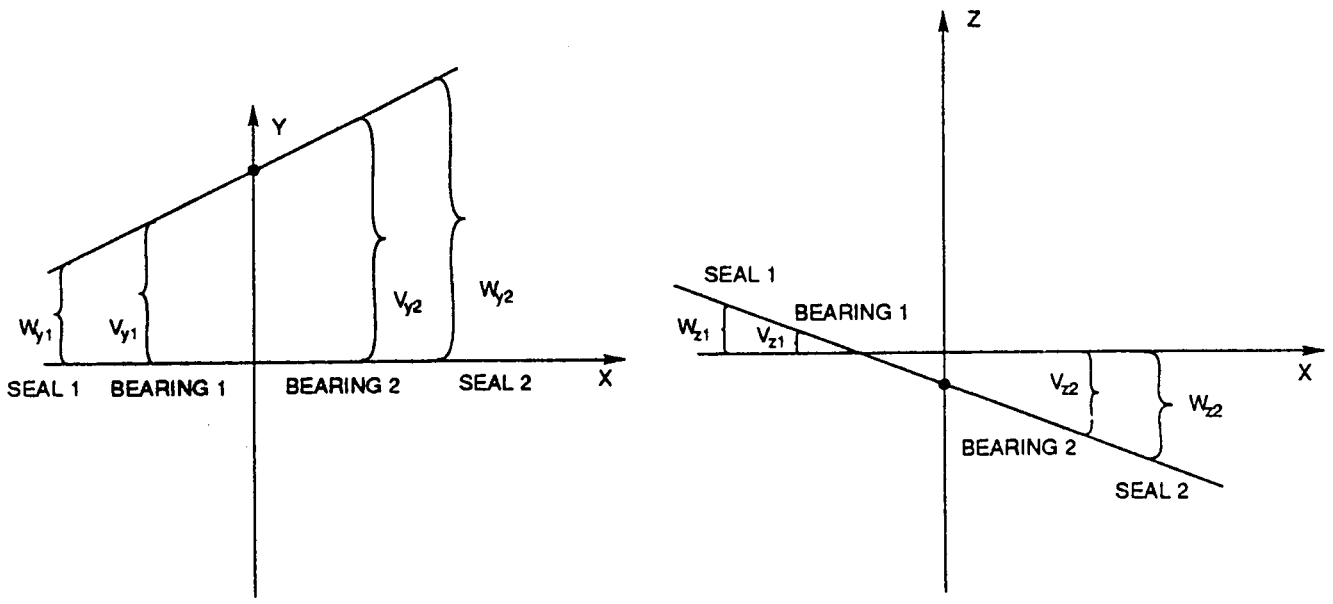
Y
X
W_{y1}
V_{y1}
V_{y2}
W_{y2}
SEAL 1
BEARING 1
BEARING 2
SEAL 2
Z
X
SEAL 1
BEARING 1
W_{z1}
V_{z1}
V_{z2}
W_{z2}
BEARING 2
SEAL 2

FIGURE 2

30000 RPM

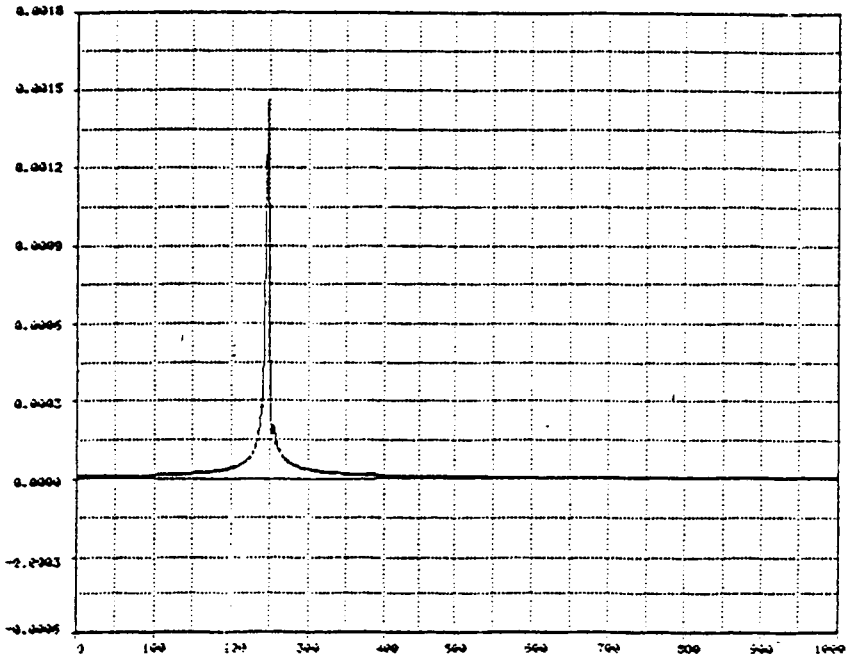

40000 RPM

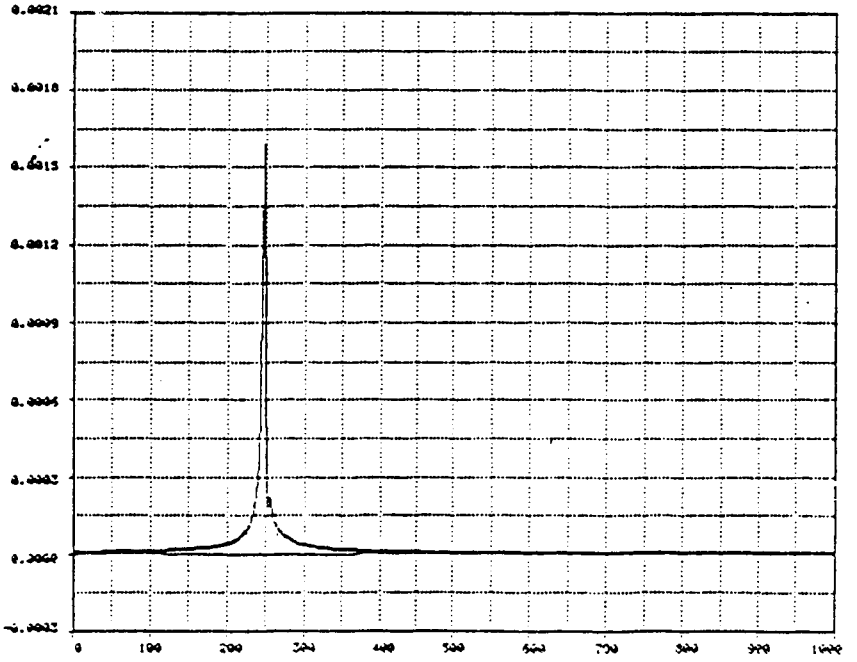

Figure 3

ORIGINAL PAGE IS
OF POOR QUALITY

50000 RPM

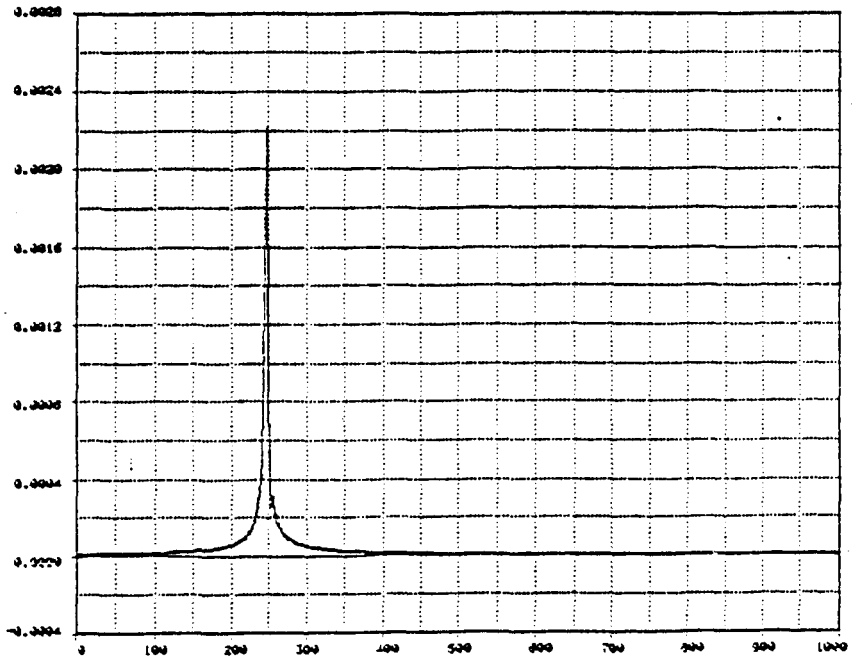

51000 RPM

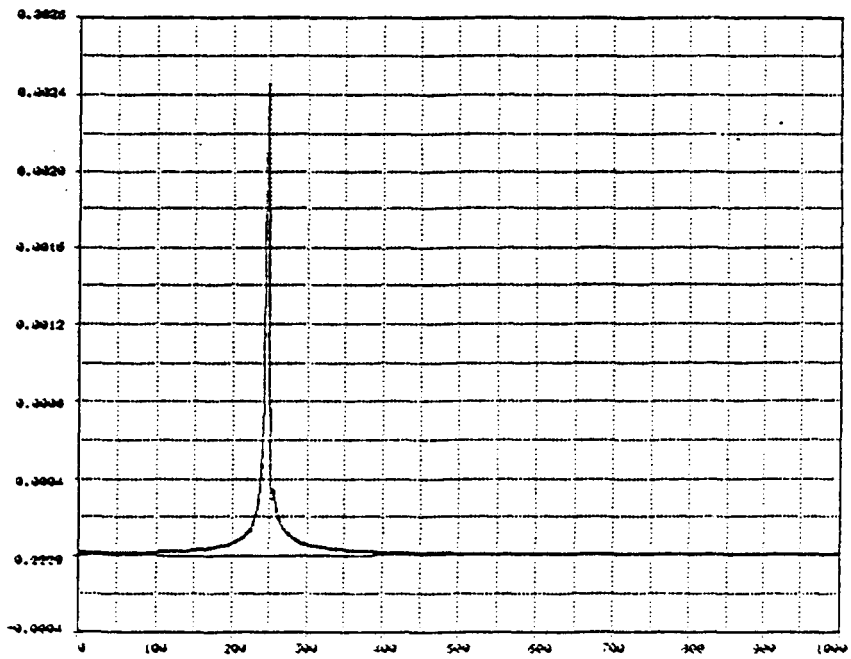

Figure 4

52000 RPM

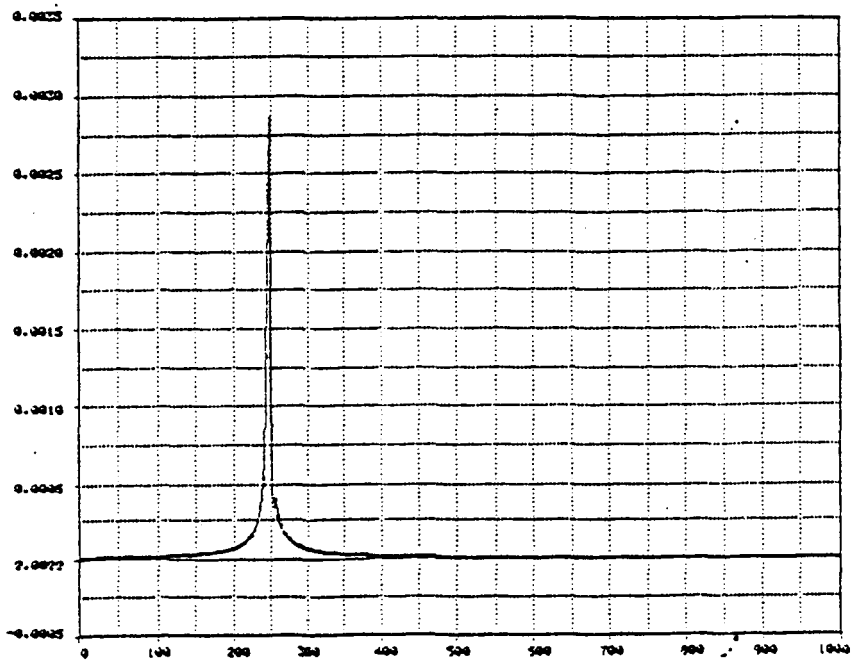

53000 RPM

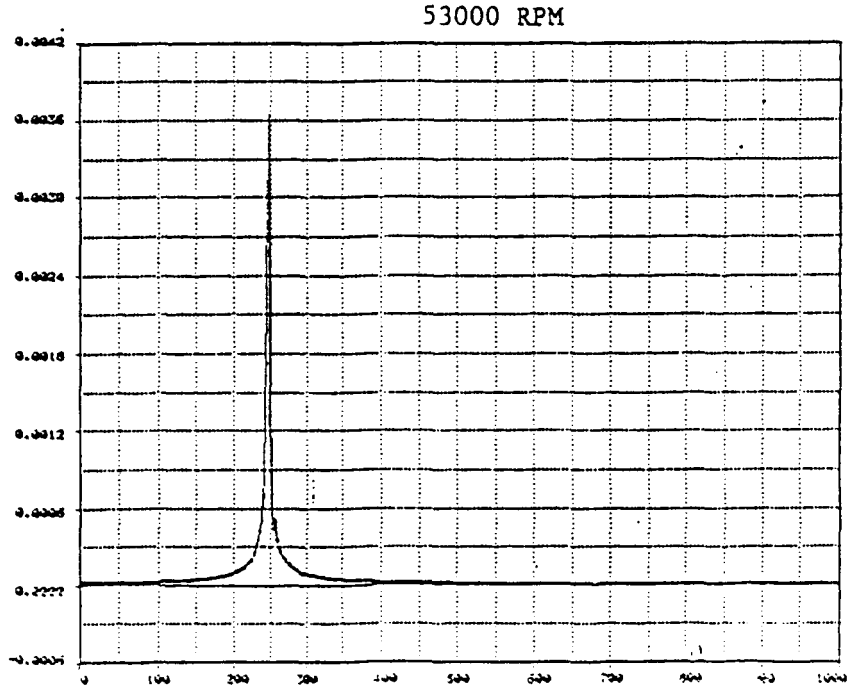

Figure 5

54000 RPM

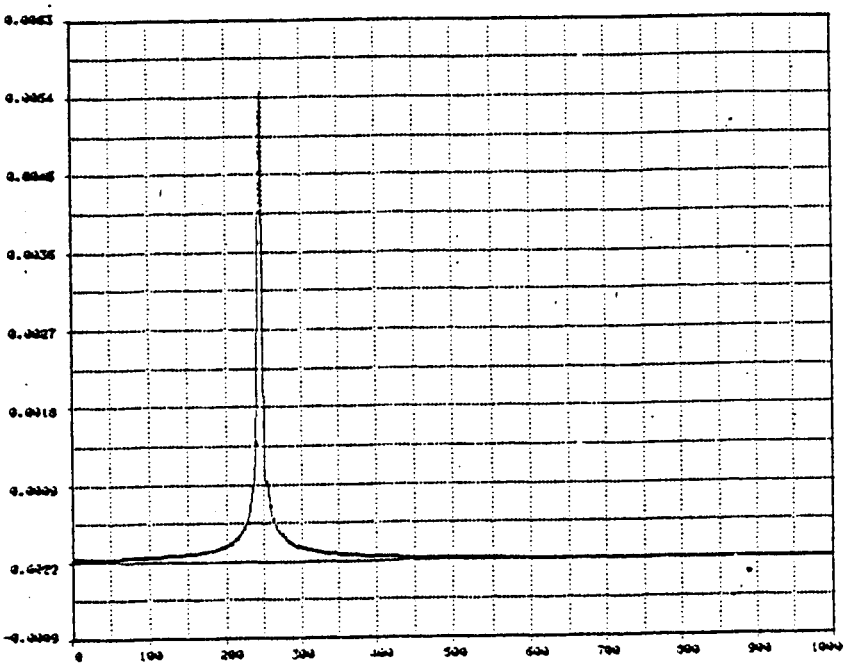

54300 RPM

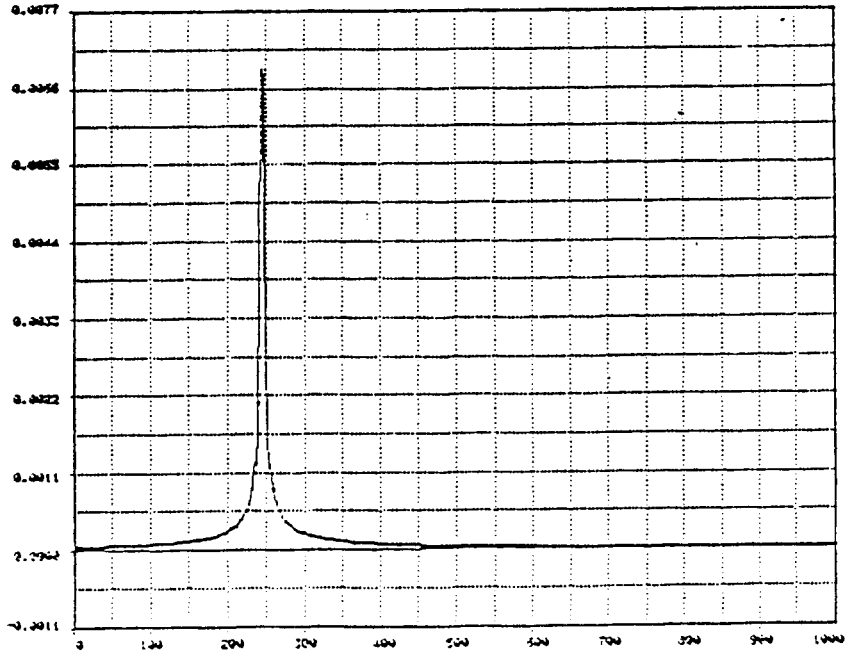

Figure 6

54600 RPM

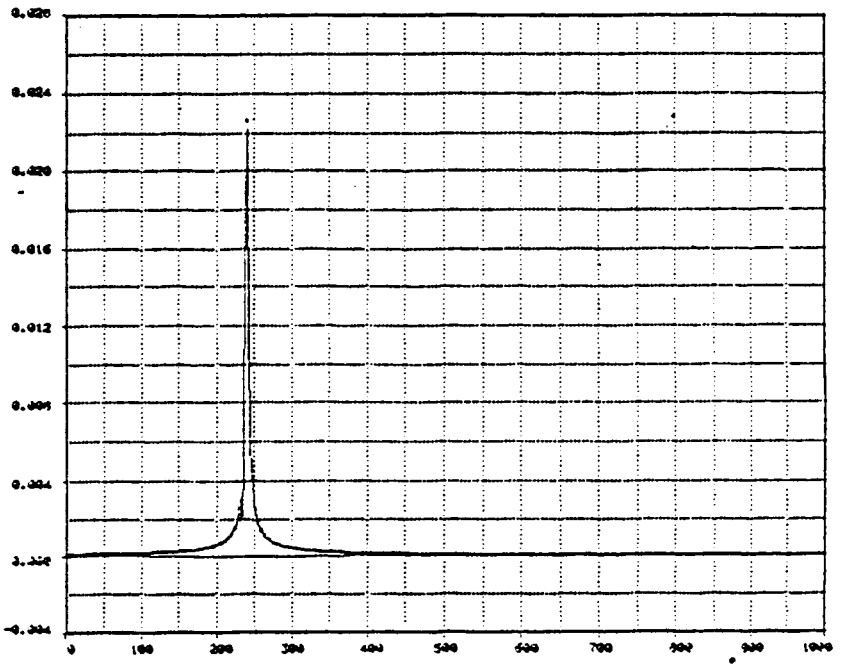

55000 RPM

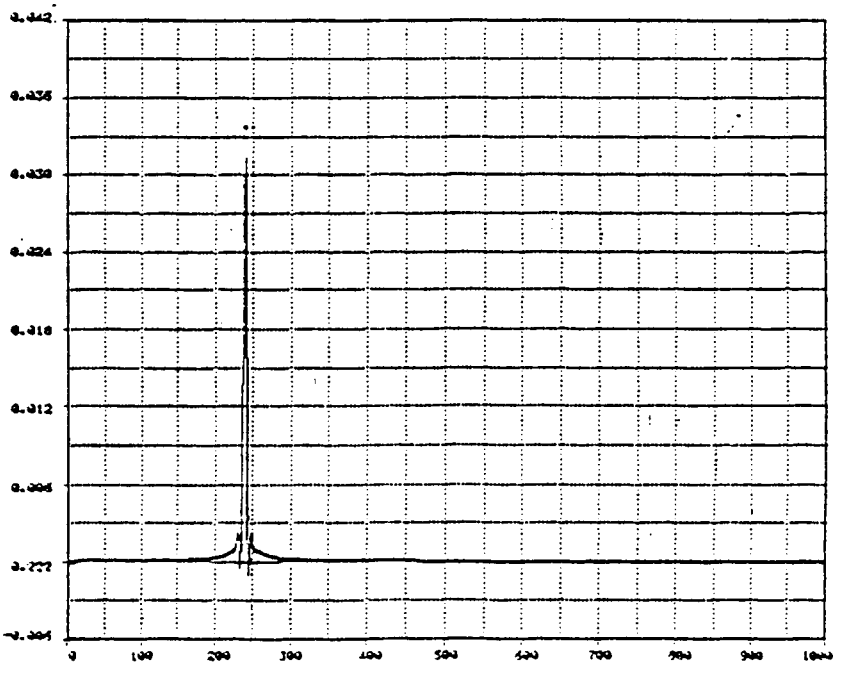

Figure 7

56000 RPM

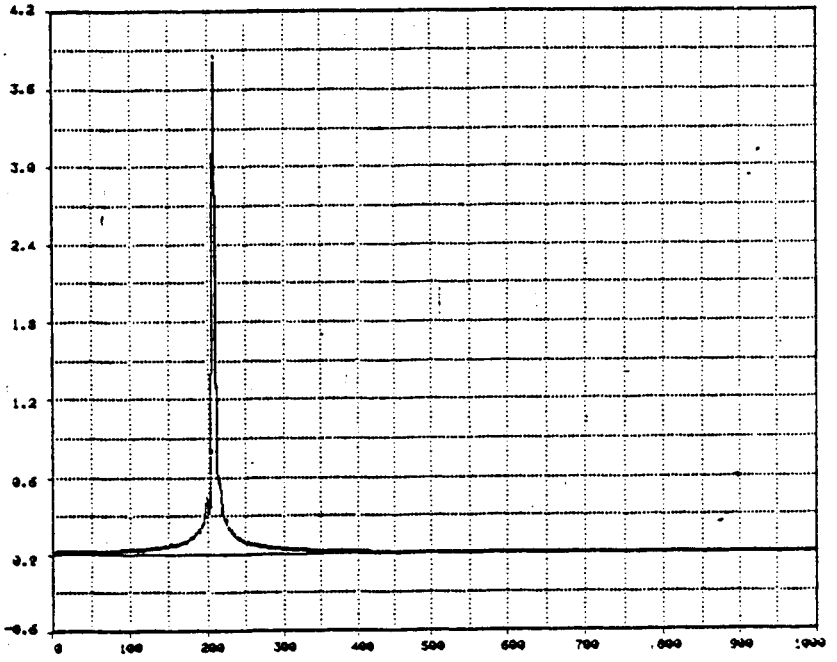

57000 RPM

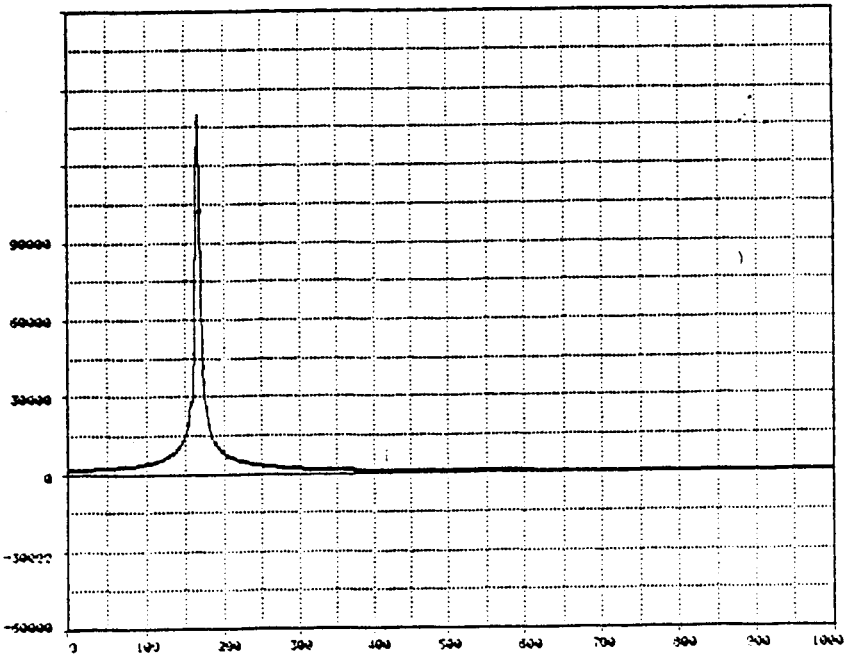

Figure 8